# Host Selection and Configuration Design of Electrophosphorescent Devices

**ARTICLE** *in* ADVANCED FUNCTIONAL MATERIALS · JULY 2007

Impact Factor: 11.81 · DOI: 10.1002/adfm.200600882



**8 AUTHORS**, INCLUDING:

Mao Li
National Institute for Materials Science
**40** PUBLICATIONS **1,176** CITATIONS
SEE PROFILE

Bing Yang
Jilin University
**74** PUBLICATIONS **1,218** CITATIONS
SEE PROFILE

Yuguang Ma
Chinese Academy of Sciences
**307** PUBLICATIONS **6,120** CITATIONS
SEE PROFILE

ADVANCED FUNCTIONAL MATERIALS



DOI: 10.1002/adfm.200600882

# Host Selection and Configuration Design of Electrophosphorescent Devices**

By *Hong Xia*, *Mao Li*, *Dan Lu*, *Chengbo Zhang*, *Weijie Xie*, *Xiaodong Liu*, *Bing Yang*, and *Yuguang Ma**

Recent studies on electrophosphorescent polymeric devices have demonstrated that charge-trapping-induced direct recombination on the phosphorescent dopant is of crucial importance. In this paper, we show that the electrochemical properties of phosphorescent molecules, which reflect their carrier-trapping ability, may be a basic design criterion for the selection of host and device configuration. The systems, consisting of a red phosphorescent $[Ru(4,7\text{-}Ph_2\text{-}phen)_3]^{2+}$ dopant and two blue hosts 2-biphenyl-4-yl-5-(4-tert-butyl-phenyl)-[1,3,4]oxadiazole (PBD) and poly(vinylcarbazole) (PVK), are intensively studied. The triplet energy level of PVK and PBD is higher than that of the $[Ru(4,7\text{-}Ph_2\text{-}phen)_3]^{2+}$, and both hosts show the ability of efficient energy transfer to the dopant, however, efficient electroluminescence (EL) is only obtained in the PVK-host system. The combined studies of photoluminescence (PL), EL, and electrochemistry for doped films demonstrate that $[Ru(4,7\text{-}Ph_2\text{-}phen)_3]^{2+}$, which undergoes a multielectron trapping process as it is used as a dopant in electron-rich (n-type) hosts, for instance, PBD, may induce an inefficient recombination for the resulting emission. Whereas using a hole-rich (p-type) polymer, such as PVK, as a host and inserting both hole-blocking and electron-transfer layers can effectively increase the efficiency of the corresponding devices up to 8.63 $Cd\,A^{-1}$, because of the reduced probability of multielectron trapping at the $[Ru(4,7\text{-}Ph_2\text{-}phen)_3]^{2+}$ sites.

## 1. Introduction

Organic light-emitting diodes (OLEDs) continue to be actively investigated because of their potential applications in, for instance, flat-panel displays.[1] The efficiency of OLEDs can be improved by the introduction of transition-metal-based phosphorescent emitters, which may harvest both singlet and triplet excitons for emission.[2,3] In phosphorescent devices, to reduce the quenching associated with relatively long excited-state lifetimes of triplet emitters and triplet–triplet annihilation, the phosphorescent emitters are normally dispersed in a conductive organic/polymer host matrix as emitting dopant guest.[3,4] The electroluminescence (EL) of the dopant results from energy transfer from the host and/or direct trapping of the charge on the phosphorescent emitter. Recent studies have shown that the direct charge trapping at the dopant sites followed by recombination with opposite charges is the dominant mechanism for phosphorescent-guest/polymer-host systems.[5] For phosphorescent OLEDs, the organic and polymer host materials must satisfy some basic conditions, such as a wide energy gap, a high charge-transport mobility, a reasonable film-forming ability, a high glass-transition temperature, etc.[6] Investigations into phosphorescent devices have indicated that the device performance is strongly dependent on the chosen host materials for the same phosphorescent dopant though these hosts all satisfy the basic conditions for host matrices.[7] Suitable host materials are very important to the efficiency of phosphorescent devices.

To match the phosphorescent guest and organic/polymer host, the current key point of view is that host materials must have a triplet energy level that is higher than the employed emitting guest. Thompson and co-workers[8] showed that the phosphorescence emission quenching is brought on by the low-energy triplet states of the fluorene-based oligomer. They demonstrated that the phosphorescent emission of $Ir^{III}$ complexes can be quenched by a polyfluorene (PF) oligomer in solution, however, for non-conjugated polymers, such as PVK, phosphorescence quenching is less favorable due to the absence of low-energy triplet states. Utilizing high-triplet-energy organic/polymer materials with a wide energy gap as the host matrix, significantly improved electrophosphorescent efficiencies were achieved for red, green, and blue heavy metal complexes.[9] Another important factor for the matching of the phosphorescent guest and organic/polymer host is the chemical compatibility between them.[10,11] Noh et al.[10] found that the phase separation of $Ir(ppy)_3$ in a PF host prevented the dopant mole-

[*] Prof. Y. G. Ma, Dr. H. Xia, M. Li, Prof. D. Lu, C. B. Zhang, W. J. Xie, Prof. X. D. Liu, Prof. B. Yang
Key Lab for Supramolecular Structure and Materials of the Ministry of Education, Jilin University
Changchun 130012 (P.R. China)
E-mail: ygma@jlu.edu.cn
Dr. H. Xia
State Key Laboratory on Integrated Optoelectronics Jilin University Region
College of Electronic Science and Engineering, Jilin University
Changchun 130012 (P.R. China)

[**] We thank both the National Science Foundation of China (grant numbers: 90501001, 20474024, 20573040, 50473001, and 60478015) and the Ministry of Science and Technology of China (grant number: 2002CB6134003).

cules from being in close proximity to the host molecules thereby inhibiting the energy-transfer process resulting in triplet–triplet annihilation. As the $Ir(ppy)_3$:PVK films were homogeneous, the good chemical compatibility of $Ir(ppy)_3$ with the PVK host results in higher efficiencies than for the PF host. The above-mentioned factors were considered in selecting phosphorescent hosts to achieve highly efficient devices. However, other factors may influence the efficiency, therefore, the continued investigation into matching the phosphorescent guest to the appropriate organic/polymer host is very necessary to guide the choosing of organic/polymer hosts and the designing of device configurations.

In this paper, we show that the electrochemical properties of the $[Ru(4,7\text{-}Ph_2\text{-}phen)_3]^{2+}$ molecule, which reflect its carrier-trapping ability, may be a basic design criterion for the selection of host materials and device configuration. The springboard for the considerable importance of the electrochemical properties of the phosphorescent dopant is based on the fact that charge trapping in dopants is a redox process, thus, the redox properties of the phosphorescent dopant (oxidation or reduction, their potentials, and reversibility) must have a great impact on the device performance. In the $Ru^{II}$ complex and organic/polymer (PVK or PBD) system triplet quenching by the host matrix cannot occur and chemical compatibility between the phosphorescent guest and host is very good. Cyclic voltammetry (CV) of the $[Ru(4,7\text{-}Ph_2\text{-}phen)_3]^{2+}$ complex shows three reversible reductive processes and one reversible oxidative process, indicating that $[Ru(4,7\text{-}Ph_2\text{-}phen)_3]^{2+}$ has the ability of trapping three electrons and only one hole. We proposed that $[Ru(4,7\text{-}Ph_2\text{-}phen)_3]^{2+}$ is undergoing a multi-electron trapping process when it is used as dopant in electron-rich (n-type) hosts, such as PBD, which may induce an inefficient recombination for the resulting emission. On the contrary, using a hole-rich (p-type) host, for instance, PVK, can reduce the probability of multi-electron trapping at the $[Ru(4,7\text{-}Ph_2\text{-}phen)_3]^{2+}$ sites, thus, the efficiency of the devices was effectively increased.

## 2. Results and Discussion

The chemical structures of the phosphorescent guest $[Ru(4,7\text{-}Ph_2\text{-}phen)_3]^{2+}$ and the two blue light-emitting hosts, namely, p-type PVK and n-type PBD, are shown in Figure 1a. The polybipyridine $Ru^{II}$ complexes are some of the most typical metal-to-ligand charge-transfer (MLCT) excited-state compounds, and the bulk of them emit red light. The $[Ru(4,7\text{-}Ph_2\text{-}phen)_3]^{2+}$ complex has a luminescence efficiency of 36%, which is the highest for Ru-based complexes.[12] As shown in Figure 1b, $[Ru(4,7\text{-}Ph_2\text{-}phen)_3]^{2+}$ shows a broad MLCT singlet absorption band centered around 460 nm and ranging between 370–520 nm and the MLCT triplet emission band is centered at 600 nm. The emission spectra of both hosts are similar with the peak wavelengths being at 410 nm and 400 nm for PVK and PBD, respectively, which overlap well with the MLCT singlet absorption band of $[Ru(4,7\text{-}Ph_2\text{-}phen)_3]^{2+}$. This overlap should enable efficient Förster energy transfer from the singlet excited state of the host to the MLCT state of the $[Ru(4,7\text{-}Ph_2\text{-}phen)_3]^{2+}$ dopant.

Figure 2 presents the degree of energy transfer that occurs between the PVK or PBD host and $[Ru(4,7\text{-}Ph_2\text{-}phen)_3]^{2+}$ dopant at doping ratios from 0.2 to 5% upon photoexcitation of the host. As can be seen in Figure 2a with PVK as a host the PL profiles of the blend contain two components: one which occurs at 355–480 nm and is a characteristic emission of the PVK host, and the second which is at 600 nm, and corresponds to the MLCT triplet emission of $[Ru(4,7\text{-}Ph_2\text{-}phen)_3]^{2+}$. The emission intensity of the PVK host was significantly reduced with an increase in the concentration of $[Ru(4,7\text{-}Ph_2\text{-}phen)_3]^{2+}$. Figure 2b shows the PL spectra of a $[Ru(4,7\text{-}Ph_2\text{-}phen)_3]^{2+}$-doped PBD film. It is clear that the PL spectra for the blends with either PVK or PBD as the host are quite similar in shape, implying that the Förster energy-transfer efficiency is almost the same for $[Ru(4,7\text{-}Ph_2\text{-}phen)_3]^{2+}$-PVK and $[Ru(4,7\text{-}Ph_2\text{-}phen)_3]^{2+}$-PBD.

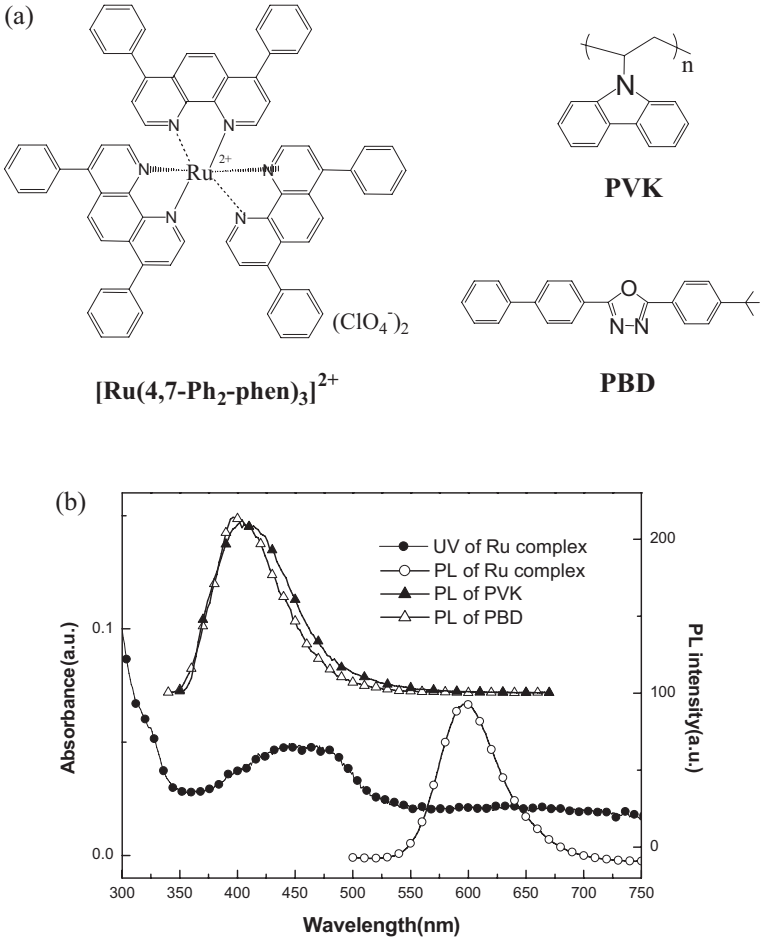


**Figure 1.** a) The molecular structures of $[Ru(4,7\text{-}Ph_2\text{-}phen)_3]^{2+}$, PVK, and PBD. b) The absorption (in $CHCl_3$) and emission (in polycarbonate film) spectra of $[Ru(4,7\text{-}Ph_2\text{-}phen)_3]^{2+}$, and the photoluminescence spectra of PVK and PBD in a neat film.

ADVANCED FUNCTIONAL MATERIALS



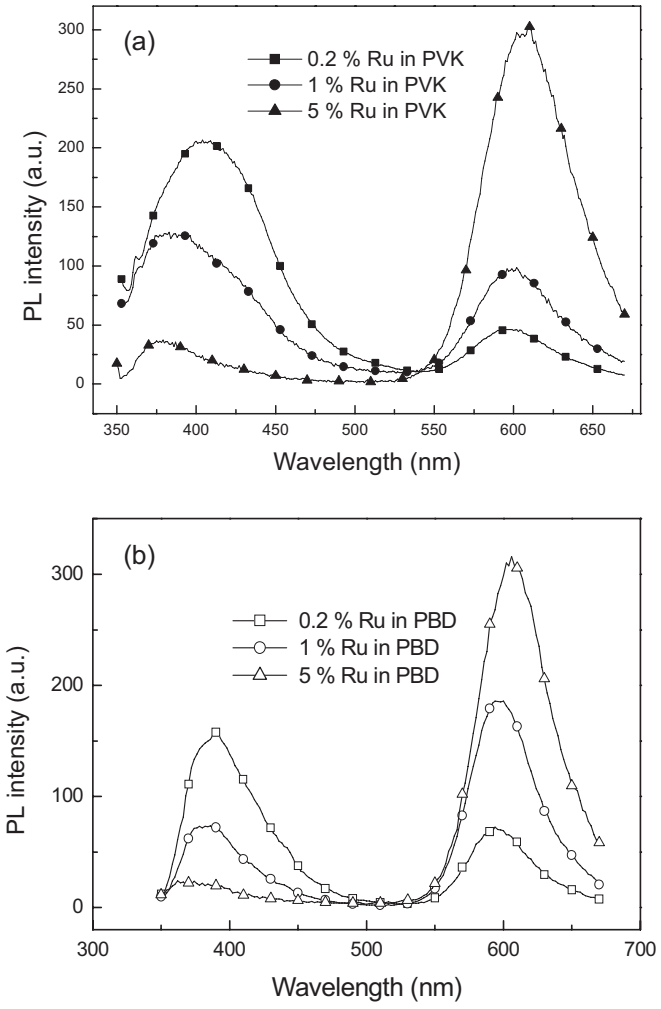


**Figure 2.** a,b) The PL spectra of $[Ru(4,7\text{-}Ph_2\text{-}phen)_3]^{2+}$-doped PVK (a) and PBD (b) film with different doping concentrations.

The surface topographies of the PVK and PBD films with 5 wt % doping concentration of $[Ru(4,7\text{-}Ph_2\text{-}phen)_3]^{2+}$ were investigated by atomic force microscopy (AFM) (Fig. 3). The $[Ru(4,7\text{-}Ph_2\text{-}phen)_3]^{2+}$-PVK and $[Ru(4,7\text{-}Ph_2\text{-}phen)_3]^{2+}$-PBD films show height variations in the range of less than ca. 3 nm and ca. 2 nm, respectively. This suggests that the blend films of PVK or PBD as host are smooth, homogeneous, and can be used for electroluminescent devices. Also, considering the efficient Förster energy transfer in both $[Ru(4,7\text{-}Ph_2\text{-}phen)_3]^{2+}$-PVK and doped PBD films we deduce that there is a good chemical compatibility between the $[Ru(4,7\text{-}Ph_2\text{-}phen)_3]^{2+}$ dopant and the PVK or PBD host.

For EL characteristics of the $[Ru(4,7\text{-}Ph_2\text{-}phen)_3]^{2+}$-doped device utilizing p-type PVK as the host, the EL spectra with varying doping concentration are shown in the inset of Figure 4. At low doping concentrations of 0.2 % and 1 % the PVK emission is present whereas at a high doping concentration of 5 % only pure red $[Ru(4,7\text{-}Ph_2\text{-}phen)_3]^{2+}$ emission can be seen. Our previous study indicated that the efficiency of a $[Ru(4,7\text{-}Ph_2\text{-}phen)_3]^{2+}$-PVK single-layer device (ITO/$Ru^{II}$:PVK/Ba/Al) is relatively low (e.g., luminance efficiency (*LE*) of 0.21 Cd $A^{-1}$), which is likely due to an imbalance of the electron and hole fluxes within the light-emitting layer. However, efficient red-light emission was obtained in multilayered-structure devices with a hole-blocking layer (2,9-dimethyl-4,7-diphenyl-[1,10]phenanthroline (BCP) or PBD) and an electron-injection layer of aluminum (tris(8-hydroxyquinolinate) ($Alq_3$)) between the cathode and the emitting layer. By optimizing the device structure and the doping concentration the device ITO/PVK:$[Ru(4,7\text{-}Ph_2\text{-}phen)_3]^{2+}$(5 %)/PBD(50 nm)/$Alq_3$(45 nm)/LiF(1.8 nm)/Al(340 nm) showed a maximum *LE* of 8.6 Cd $A^{-1}$ at a current density of 0.05 mA $cm^{-2}$ and at a brightness of 4.1 Cd $m^{-2}$. The *LE* value is approximately 6.0 Cd $A^{-1}$ at higher current density and brightness (Figure 4). The $[Ru(4,7\text{-}Ph_2\text{-}phen)_3]^{2+}$-PVK devices with a BCP hole-blocking layer can also achieve a $LE_{max}$ of 4.1 Cd $A^{-1}$.

However, when used as dopant in the n-type PBD host, the $Ru^{II}$ complex luminance efficiency is not as high as when using the p-type PVK as the host. The optimized dopant concentration for the device ITO/PEDOT:PSS/$Ru^{II}$:PBD/Ba/Al was 5 wt %, the $LE_{max}$ for this device is 0.086 Cd $A^{-1}$ at a current density (*J*) of 30 mA $cm^{-2}$, and the maximum brightness ($B_{max}$) of the device is 50 Cd $m^{-2}$ at an applied voltage (*V*) of 13 V (PEDOT: poly(3,4-ethylenedioxythiophene); PSS poly(styrenesulfonate). The relatively low efficiency of a $[Ru(4,7\text{-}Ph_2\text{-}phen)_3]^{2+}$:PBD single-layer device is likely due to lower hole-injection efficiency which induces a poor balance of the electron and hole within the device. A significant enhancement in device efficiency was achieved by inserting PVK as a hole-injection and transport layer between the PEDOT:PSS and $Ru^{II}$:PBD layers. Table 1 lists detailed performance data for devices ITO/PEDOT:PSS/PVK/(5 %)$[Ru(4,7\text{-}Ph_2\text{-}phen)_3]^{2+}$:PBD/Ba/Al with different concentrations of PVK in $CHCl_3$ solution ranging from 1 mg $mL^{-1}$ to 4 mg $mL^{-1}$. The *LE*–*J* characteristics of the 5 % $[Ru(4,7\text{-}Ph_2\text{-}phen)_3]^{2+}$-doped PBD multilayer device is shown in Figure 5. The *B* and *LE* of these multilayer devices is higher than that of a single-layer device for the PBD host, and the device with a hole-injection layer consisting of PVK at a concentration of 3 mg $mL^{-1}$ gives the highest EL efficiency of 0.96 Cd $A^{-1}$ at a *J* of 5.88 mA $cm^{-2}$. The inset of Figure 5 shows the EL spectra of devices with PBD as host. At 1 % and 5 % $[Ru(4,7\text{-}Ph_2\text{-}phen)_3]^{2+}$ doping concentration the PBD emission is absent, only pure red $[Ru(4,7\text{-}Ph_2\text{-}phen)_3]^{2+}$ emission is seen. For devices with PVK or PBD as a host and $[Ru(4,7\text{-}Ph_2\text{-}phen)_3]^{2+}$ as a dopant the coordinates on the Commission Internationale de l'Eclairage

**Table 1.** Performance of devices of ITO/PEDOT:PSS/(*x* mg $mL^{-1}$) PVK/(5 wt %)$[Ru(4,7\text{-}Ph_2\text{-}phen)_3]^{2+}$:PBD/Ba/Al, x = 1, 2, 3 and 4.

| Conc. of PVK [mg $mL^{-1}$] | Turn-on voltage [V] | $B_{max}$ [Cd $m^{-2}$] | $LE_{max}$ [Cd $A^{-1}$] | CIE (1931) (*x*,*y*) |
|---|---|---|---|---|
| 1 | 12.0 | 107 | 0.34 | 0.62,0.37 |
| 2 | 12.5 | 127 | 0.61 | 0.62,0.37 |
| 3 | 13.0 | 183 | 0.96 | 0.63,0.37 |
| 4 | 15.0 | 154 | 0.70 | 0.63,0.37 |

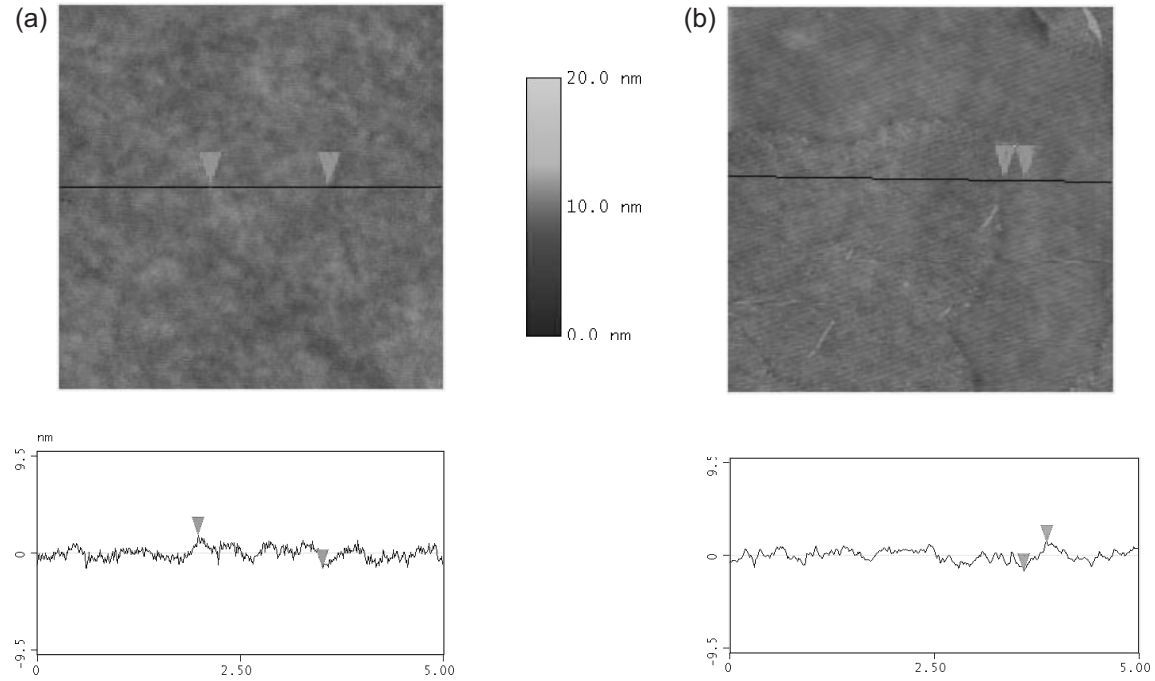


**Figure 3.** a,b) AFM images (5 μm × 5 μm) of films of (5 %) $[Ru(4,7\text{-}Ph_2\text{-}phen)_3]^{2+}$-PVK (a) and (5 %) $[Ru(4,7\text{-}Ph_2\text{-}phen)_3]^{2+}$-PBD (b).

(CIE 1931) chromaticity chart are similar (0.62, 0.37). However, there is a clear difference in device efficiency, devices fabricated with a PVK host showed a significant increase in *LE* (8.6 Cd $A^{-1}$) over devices with a PBD host (0.96 Cd $A^{-1}$).

In order to clarify the reasons inducing these significant differences in performance of devices with PVK and PBD hosts, we review the properties of both PVK and PBD hosts and some properties correlating with host–dopant interactions. It is known that both PVK and PBD hosts possess similar emission spectra (Fig. 1b), and almost equal energy gaps (as calculated by the absorbance band edge) of 3.5 eV (PVK) and 3.6 eV (PBD). Both hosts also show efficient Förster energy transfer, have a good film quality and chemical compatibility for $[Ru(4,7\text{-}Ph_2\text{-}phen)_3]^{2+}$-doped blend films (Figs. 2 and 3). The triplet energy levels of PVK (2.5 eV) and PBD (2.54 eV) are higher than that of $[Ru(4,7\text{-}Ph_2\text{-}phen)_3]^{2+}$ (2.07 eV) and the phosphorescence quenching is less favorable due to the absence of any low-energy triplet states.[13,8] The largest difference between the PVK and PBD host is their different charge-carrier transfer ability, namely, PVK is a p-type host, and PBD is an n-type host. This implies that holes are the main charge carriers for the PVK host and electrons are the main charge carriers for the PBD host in the respective light-emitting layers. Further, to explain the effect of majority carrier type on device performance, we studied the electrochemical behavior of the Ru complex and both hosts and found that the electrochemical charge-trapping ability of the dopant plays an important role in selecting the host material.

Figure 6 illustrates CV curves for $[Ru(4,7\text{-}Ph_2\text{-}phen)_3]^{2+}$, PVK and PBD. The $[Ru(4,7\text{-}Ph_2\text{-}phen)_3]^{2+}$ complex shows reversible oxidation and reduction processes, which implies a strong charge-trapping ability of the $Ru^{II}$ guest and a potential improvement in the stability of electroluminescent devices.[14] Three reduction waves and only one oxidation wave could be observed for $[Ru(4,7\text{-}Ph_2\text{-}phen)_3]^{2+}$, which means that $[Ru(4,7\text{-}Ph_2\text{-}phen)_3]^{2+}$ has the ability of trapping three electrons and only one hole. These reduction and oxidation processes take place on the ligand π*-orbitals and metal-centered orbital, respectively. The reduction and oxidation onset potentials of $[Ru(4,7\text{-}Ph_2\text{-}phen)_3]^{2+}$ are –1.47, –1.67, –1.86, and 0.78 V (V versus $Ag/Ag^+$), respectively (Table 2). The HOMO and LUMO levels of $[Ru(4,7\text{-}Ph_2\text{-}phen)_3]^{2+}$, PVK, and PBD were obtained through CV and absorbance-band-edge studies (Figs. 7 and 8). Recent reports on polymer-host/phosphorescent-dopant systems have demonstrated that charge-trapping-induced direct recombination on the phosphorescent dopant site is of crucial importance.[5] The LUMO levels of PVK and PBD hosts are higher than that of $[Ru(4,7\text{-}Ph_2\text{-}phen)_3]^{2+}$, and their HOMO levels are lower than that of $[Ru(4,7\text{-}Ph_2\text{-}phen)_3]^{2+}$, thus, the $[Ru(4,7\text{-}Ph_2\text{-}phen)_3]^{2+}$ molecule should be efficient at trapping holes and electrons from the hosts. The dif-

**Table 2.** Redox potentials ($E_{1/2}$) versus $Ag/Ag^+$(0.01 M) of $Ru(4,7\text{-}Ph_2\text{-}phen)_3]^{2+}$ complex, PVK, and PBD.

| | Oxidation $E_{onset}$ [V] | | | Reduction $E_{onset}$ [V] | | $\Delta E_{onset}$ [V] |
|---|---|---|---|---|---|---|
| | 0/1+ | 2+/3+ | 2+/1+ | 1+/0 | 0/1– | – |
| Ru(dpp) | – | 0.76 | –1.47 | –1.67 | –1.86 | 2.23 |
| PVK | 0.79 | – | – | – | –2.71 | 3.50 |
| PBD | – | – | – | – | –2.22 | – |

ADVANCED FUNCTIONAL MATERIALS



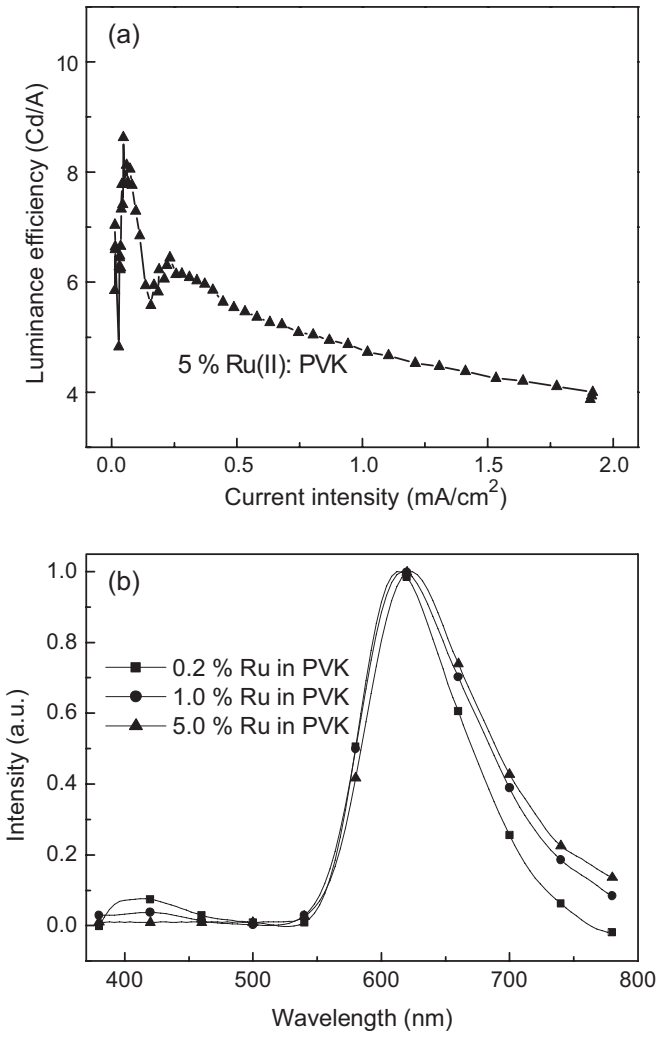


**Figure 4.** a) The LE versus current density of device ITO/PVK:[Ru(4,7-$Ph_2$-phen)$_3$]$^{2+}$(5 wt %)/PBD(50 nm)/$Alq_3$(45 nm)/LiF(1.8 nm)/Al(340 nm). b) EL spectra of single-layer device ITO/PVK:*x* % Ru(4,7-$Ph_2$-phen)$_3$]$^{2+}$/LiF/Al.

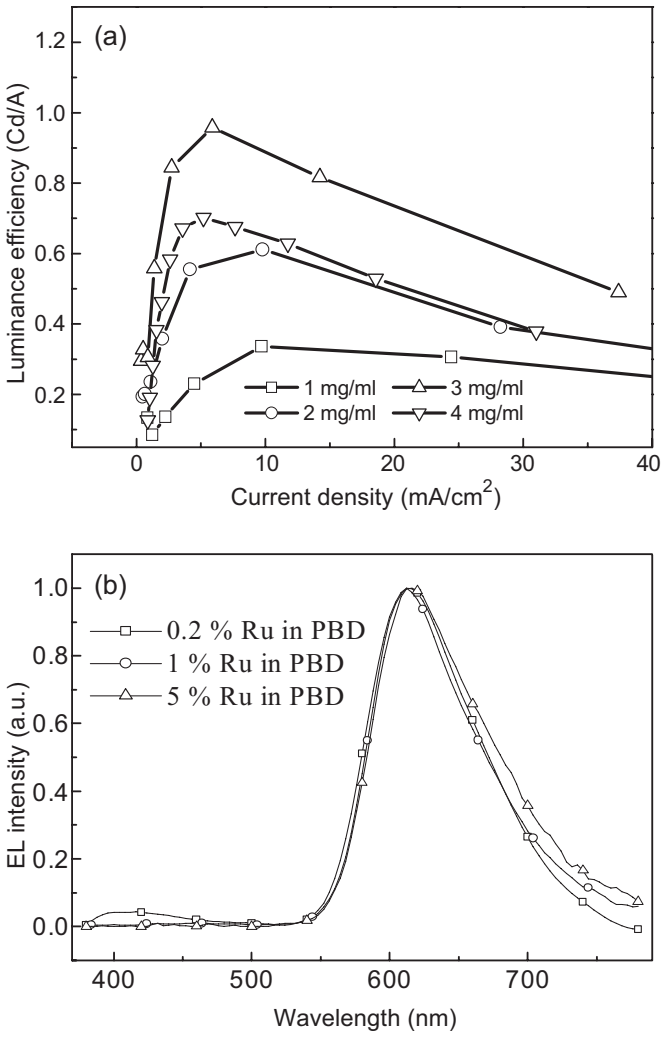


**Figure 5.** a) The luminance efficiency versus current density of device ITO/(*x* mg mL$^{-1}$) PVK/PEDOT:PSS/(5 %)[Ru(4,7-$Ph_2$-phen)$_3$]$^{2+}$:PBD/Ba/Al, *x* = 1, 2, 3, or 4. b) EL spectra of device ITO/PEDOT:PSS/(*x* %) Ru(4,7-$Ph_2$-phen)$_3$]$^{2+}$:PBD/Ba/Al, *x*= 0.2, 1, or 5 %.

ferent charge-transport abilities of the hosts (PBD and PVK) and the special electrochemical behavior of [Ru(4,7-$Ph_2$-phen)$_3$]$^{2+}$ molecule are the reasons for the great contrast between the OLED performances of the devices with PVK or PBD as a host.

The band structure and charge-trapping processes in the light-emitting layer with PBD as a host are shown in Figure 7. As an electric field is applied to devices with [Ru(4,7-$Ph_2$-phen)$_3$]$^{2+}$-doped PBD as the light-emitting layer electrons become the main charge carriers in the light-emitting layer. The CV curve of [Ru(4,7-$Ph_2$-phen)$_3$]$^{2+}$ showed that the [Ru(4,7-$Ph_2$-phen)$_3$]$^{2+}$ guest has a good electron-trapping ability, and the highest number of trapped electrons is three for each [Ru(4,7-$Ph_2$-phen)$_3$]$^{2+}$ molecule in the potential range available. According to the energy-band diagram (Fig. 7), the three unoccupied molecular orbits (–2.77, –2.96, –3.16 eV) of [Ru(4,7-$Ph_2$-phen)$_3$]$^{3+}$ are lower than the LUMO (–2.55 V) of the PBD host. The electrons that inhabit the LUMO of the PBD polymer host can be trapped by three unoccupied molecular orbits of [Ru(4,7-$Ph_2$-phen)$_3$]$^{2+}$ molecules and the reduced states of the complex may be formed. Each [Ru(4,7-$Ph_2$-phen)$_3$]$^{2+}$ molecule may trap one, two, or three electrons from the PBD host matrix at the drive voltage, and the reduced states [$Ru^{2+}L_2L^-$]$^+$, [$Ru^{2+}L(L^-)_2$], or [$Ru^{2+}(L^-)_3$]$^-$ may be formed (Scheme 1(1)). While the holes are injected into the

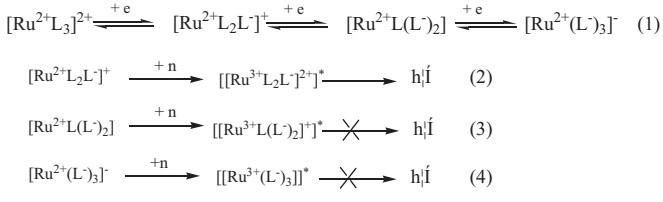


**Scheme 1.** The processes of electron and hole recombination and deactivation of excited states in the light-emitting layer with PBD as host.

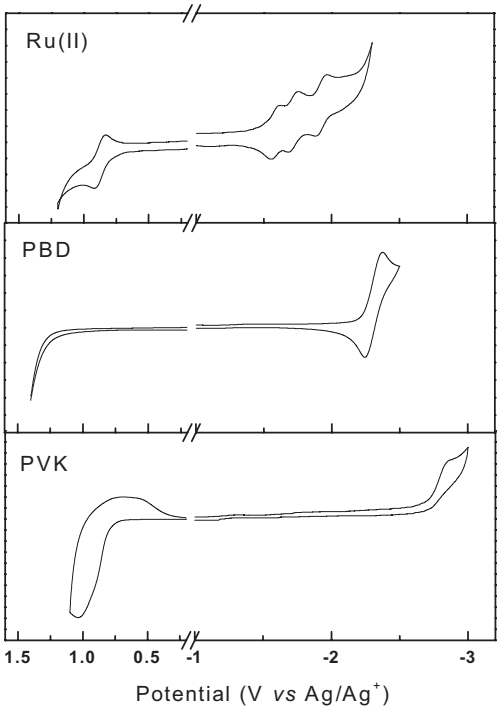


**Figure 6.** CV curves of $[Ru(4,7\text{-}Ph_2\text{-}phen)_3]^{2+}$, PBD, and PVK.

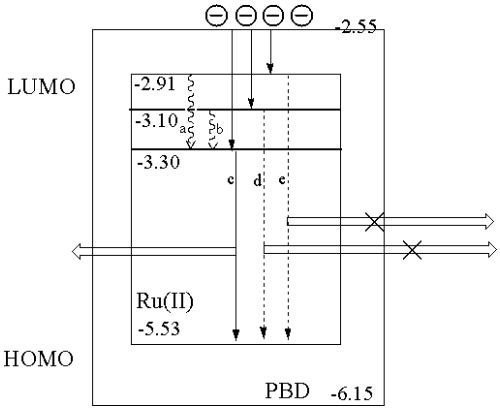


**Figure 7.** HOMO and LUMO levels for materials and charge-trapping diagram in light-emitting layer with PBD as host.

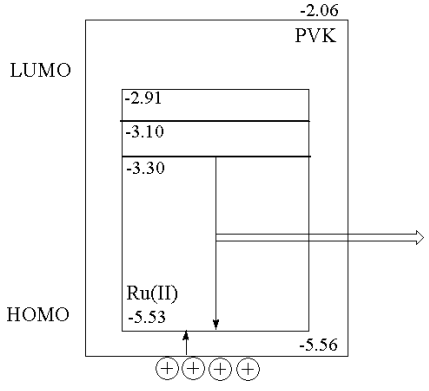


**Figure 8.** HOMO and LUMO levels for materials and charge-trapping diagram in light-emitting layer with PVK as host.

light-emitting layer from the ITO anode, recombination of holes and reduced states of the $[Ru(4,7\text{-}Ph_2\text{-}phen)_3]^{2+}$ molecule occurs and, so, excited states are formed. If there is only the first reduced state $[Ru^{2+}L_2L^-]^+$, that is, the $[Ru(4,7\text{-}Ph_2\text{-}phen)_3]^{2+}$ molecule only trapped one electron, even though this electron was at a higher energy unoccupied molecular orbital, it can decay to the lowest energy unoccupied molecular orbital (processes a and b in Figure 7) by non-radiant transition, and an according excited state $[[Ru^3L_2(L^-)]^{2+}]^*$ will release energy as radiation luminescence (process c in Figure 7 and in Scheme 1(2)). But if the number of trapped electrons was two or three for one $[Ru(4,7\text{-}Ph_2\text{-}phen)_3]^{2+}$ molecule, in other words, if the reduced states $[Ru^{2+}L(L^-)_2]$ and $[Ru^{2+}(L^-)_3]^-$ are formed, these can recombine with holes from the anode, and the high-energy excited states $[[Ru^{3+}L(L^-)_2]^+]^*$ and $[[Ru^{3+}(L^-)_3]]^*$ are formed. These high-energy excited states of transition-metal complexes undergo radiationless deactivation (processes d and e in Figure 7 and in Scheme 1(3,4)).[15] It can be deduced from this that the luminescent emission is efficient only if a single electron is trapped by the $[Ru(4,7\text{-}Ph_2\text{-}phen)_3]^{2+}$ molecules. If more electrons are trapped, the charge carriers cannot efficiently be utilized in the devices with $[Ru(4,7\text{-}Ph_2\text{-}phen)_3]^{2+}$:PBD blend as light-emitting layer and the device performance is poor.

The electron-transfer material is not suited as a host for $[Ru(4,7\text{-}Ph_2\text{-}phen)_3]^{2+}$ devices. The substitution of the electron-transfer host for a hole-transfer host is necessary, which can dramatically reduce the electron accumulation at the sites of the reduced states of $[Ru(4,7\text{-}Ph_2\text{-}phen)_3]^{2+}$, and the performance of the Ru-complex PLEDs can be remarkably enhanced.

The CV curve of $[Ru(4,7\text{-}Ph_2\text{-}phen)_3]^{2+}$ shows only one reversible oxidation process, which implies that it cannot form a higher oxidation state (Scheme 2(1)). During the operation of devices with PVK as a host holes are the main carriers in the

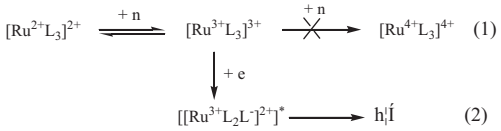


**Scheme 2.** The processes of electron and hole recombination and deactivation of excited states in the light-emitting layer with PVK as host.

light-emitting layer and the $[Ru(4,7\text{-}Ph_2\text{-}phen)_3]^{2+}$ complex behaves as a hole trap. A recombination in the light-emitting layer of the oxidation state $[Ru^{3+}L_3]^{3+}$ and electrons from the cathode occurs and the formed excitons, $[[Ru^{3+}L_2L^-]^{2+}]^*$, undergo radiation luminescence (Scheme 2(2)). It is evident that the probability of radiationless decay of $[Ru(4,7\text{-}Ph_2\text{-}phen)_3]^{2+}$ is reduced significantly with PVK as a host. The matching of the electrochemical behavior of the dopant and the carrier transfer ability of the host is, thus, an important factor to enhancing the performance of PLEDs.

The carrier-transport ability of the host can observably influence the performance of the $[Ru(4,7\text{-}Ph_2\text{-}phen)_3]^{2+}$ emitter in

ADVANCED FUNCTIONAL MATERIALS



electrophosphorescent devices, because of the special charge-carrier-trapping ability of the guest. In order to understand this matter further, a blend of PVK and PBD was selected as a host matrix for the $Ru^{II}$ complex guest. The carrier-transport ability of the host can be gradually changed by adjusting the ratio of PVK and PBD in the blend. Table 3 displays the device performance of ITO/PEDOT:PSS/(0.5 %)[Ru(4,7-$Ph_2$-phen)$_3$]$^{2+}$:PVK–PBD($x$ %)/Ba/Al with varying concentrations of PBD in the PVK–PBD blend from 5 wt % to 80 wt %. As a result, these devices exhibited $LE_{max}$ ranging from 0.041 Cd $A^{-1}$ to 3.0 Cd $A^{-1}$, maximum brightness ranging from 38 Cd $m^{-2}$ to 2692 Cd $m^{-2}$, and turn-on voltages in the range of 11.0 V to 7.6 V. The performance of devices with a [Ru(4,7-$Ph_2$-phen)$_3$]$^{2+}$ emitter was the best when the concentration of PBD was 40 wt % in the PVK–PBD blend, implying that for this blend the carrier-transporting ability of the host matches the electrochemical properties of [Ru(4,7-$Ph_2$-phen)$_3$]$^{2+}$ molecule the most. Meanwhile, a $LE_{max}$ of 5.71 Cd $A^{-1}$ was achieved for the device ITO/PEDOT:PSS/[Ru(4,7-$Ph_2$-phen)$_3$]$^{2+}$:PVK–PBD (40 wt %)/Ba/Al by adjusting the [Ru(4,7-$Ph_2$-phen)$_3$]$^{2+}$ concentration in the PVK–PBD (40 wt %) host to 0.8 wt %.

**Table 3.** Performance of devices of ITO/PEDOT:PSS/($x$ mg $mL^{-1}$) PVK/$Ru^{II}$:PVK-PBD($x$ wt %)/Ba/Al.

| [Ru(II)] [%] | PBD [wt %] | Turn-on [V] | $B_{max}$ [Cd $m^{-2}$] | $LE_{max}$ [Cd $A^{-1}$] | $PE_{max}$ [lm $W^{-1}$] | CIE (1931) ($x$,$y$) |
|---|---|---|---|---|---|---|
| 0.5 | 5 | 11.0 | 38 | 0.041 | 0.012 | 0.48,0.31 |
| 0.5 | 20 | 8.4 | 666 | 0.78 | 0.22 | 0.59,0.37 |
| 0.5 | 40 | 7.6 | 2692 | 3.00 | 0.83 | 0.60,0.37 |
| 0.5 | 60 | 8.0 | 1637 | 2.27 | 0.65 | 0.59,0.36 |
| 0.5 | 80 | 9.8 | 153 | 0.85 | 0.19 | 0.54,0.34 |
| 0.8 | 40 | 7.8 | 2286 | 5.71 | 1.91 | 0.60,0.37 |

For most heavy-metal (e.g., Ir, Pt, Re) complexes, the electrochemical behavior shows similar multi-reduction and single-oxidation processes as observed for [Ru(4,7-$Ph_2$-phen)$_3$]$^{2+}$. So, p-type materials, for example, PVK, CBP, and their derivatives, are widely used as host matrices to avoid multi-electron trapping, and multilayer structures with a hole-blocking layer and electron-injection layer are needed for the carrier balance of electrons and holes.

## 3. Conclusions

The CV curves of [Ru(4,7-$Ph_2$-phen)$_3$]$^{2+}$ show that the [Ru(4,7-$Ph_2$-phen)$_3$]$^{2+}$ molecule has four reversible redox processes, i.e., three electroreduction processes and one electrooxidation process. The electrochemical properties of the [Ru(4,7-$Ph_2$-phen)$_3$]$^{2+}$ molecule, which reflects the carrier-trapping ability of the guest, may be a basic design criterion for the selection of polymer matrices and device configuration. When an n-type polymer such as PBD is used as a host, the excess electrons can easily be trapped forming three reduced states of the Ru complex, however, radiationless deactivation of high-energy excited states occurs, so the device performance was poor. Whereas if a hole-transfer material is used as a host and a hole-blocking layer is inserted, the probability of multi-electron trapping at the [Ru(4,7-$Ph_2$-phen)$_3$]$^{2+}$ sites is reduced, thus, increasing the efficiency of the devices. Devices with a [Ru(4,7-$Ph_2$-phen)$_3$]$^{2+}$–PVK blend as the light-emitting layer achieved high luminance efficiencies up to 8.6 Cd $A^{-1}$.

## 4. Experimental

The synthesis of [Ru(4,7-$Ph_2$-phen)$_3$]$^{2+}$ was reported elsewhere [16]. PVK, PBD, 2,9-dimethyl-4,7-diphenyl-[1,10]phenanthroline (BCP), and $Al^{III}$ tris(8-hydroxyquinolinate) ($Alq_3$), were purchased from Aldrich and used without further purification.

UV-vis absorption spectra were recorded on a UV-3100 spectrophotometer. Fluorescence measurements were carried out with a RF-5301PC. The films for PL experiments were prepared on pre-cleaned quartz plates in air atmosphere.

Electrochemical measurements were performed with a BAS 100W Bioanalytical Systems, using a platinum disk ($\varphi = 2$ mm) as working electrode, platinum wire as auxiliary electrode, and a porous glass wick $Ag/Ag^+$ as reference electrode. Cyclic voltammetry (CV) studies of the [Ru(4,7-$Ph_2$-phen)$_3$]$^{2+}$ complex were carried out at a scan rate of 50 mV $s^{-1}$ and in dimethylformamide (DMF) solutions containing 0.1 M $NBu_4BF_4$ as supporting electrolyte. CV studies of the PBD and PVK solid films were carried out at a scan rate of 50 mV $s^{-1}$ and in acetonitrile solutions containing 0.1 M $NBu_4PF_6$ as supporting electrolyte. Using the onset potentials in the CV curves, the LUMO (lowest unoccupied molecular orbital) and HOMO (highest occupied molecular orbital) energy levels of the material were determined; and using the difference between the LUMO and HOMO, the energy gap of the materials was estimated.

Indium-tin-oxide (ITO)-coated glass with a sheet resistance of $< 50\Omega$/sq. was used as substrate. The substrate was pre-patterned by photolithography to give an effective device size of 4 $mm^2$. Active layers were spin-coated from 10 mg $mL^{-1}$ chloroform solutions of 0.5–5.0 % (w/w) [Ru(4,7-$Ph_2$-phen)$_3$]$^{2+}$ in the host (PVK or PBD) at a speed of 3000 rpm on ITO substrates to give a film thickness of 80–100 nm. The hole-blocking and electron-injection layers were deposited by thermo-evaporation. A cathode consisting of LiF (1.8 nm)/Al (340 nm) or Ba (5 nm)/Al (340 nm) was deposited. The luminance ($B$)–current density ($J$)–voltage (V) characteristics were recorded by combining the PR650 spectroscan spectrometer with a Keithley model 2400 programmable voltage–current source. The electroluminescent (EL) spectra and Commission Internationale de L'Eclairage (CIE) coordinates of the devices were measured by a PR650 spectroscan spectrometer. These measurements were made at room temperature and under ambient conditions.

Received: September 26, 2006
Revised: December 31, 2006
Published online: June 20, 2007

[1] a) C. W. Tang, S. A. Van Slyke, *Appl. Phys. Lett.* **1987**, *51*, 913. b) J. H. Burroughes, D. D. C. Bradley, A. R. Brown, R. N. Makers, K. Mackay, R. H. Friend, P. L. Burn, A. B. Holmes, *Nature* **1990**, *347*, 539.

[2] a) Y. G. Ma, H. Y. Zhang, C. M. Che, J. C. Shen, *Synth. Met.* **1998**, *94*, 245. b) Y. Cao, I. D. Parker, G. Yu, C. Zhang, A. J. Heeger, *Nature* **1999**, *397*, 414. c) M. A. Baldo, D. F. O'Brien, Y. You, A. Shoustikov, S. Sibley, M. E. Thompson, S. R. Forrest, *Nature* **1998**, *395*, 151.

[3] a) C. Adachi, M. A. Baldo, S. R. Forrest, *Appl. Phys. Lett.* **2000**, *77*, 904. b) X. Gong, W. Ma, J. C. Ostrowski, K. Bechgaard, G. C. Bazan, A. J. Heeger, S. Xiao, D. Moses, *Adv. Funct. Mater.* **2004**, *14*, 393. c) X. Gong, M. R. Robinson, J. C. Ostrowski, D. Moses, G. C. Bazan, A. J. Heeger, *Adv. Mater.* **2002**, *14*, 581. d) Y. L. Tung, L. S. Chen,

  

Y. Chi, P. T. Chou, Y. M. Cheng, E. Y. Li, G. H. Lee, C. F. Shu, F. I. Wu, A. J. Carty, *Adv. Funct. Mater.* **2006**, *16*, 1615. e) Y. G. Ma, C. M. Che, W. H. Chen, X. M. Zhou, J. C. Shen, *Adv. Mater.* **1999**, *11*, 852. f) J. Kavitha, S. Y. Chang, Y. Chi, J. K. Yu, Y. H. Hu, P. T. Chou, S. M. Peng, G. H. Lee, Y. T. Tao, C. H. Chien, A. J. Carty, *Adv. Funct. Mater.* **2005**, *15*, 223. g) H. Xia, C. B. Zhang, S. Qiu, P. Lu, J. Y. Zhang, Y. G. Ma, *Appl. Phys. Lett.* **2004**, *84*, 290. h) H. Xia, C. B. Zhang, X. D. Liu, S. Qiu, P. Lu, F. Z. Shen, J. Y. Zhang, Y. G. Ma, *J. Phys. Chem. B* **2004**, *108*, 3185.

[4] a) C. Y. Jiang, W. Yang, J. B. Peng, S. Xiao, Y. Cao, *Adv. Mater.* **2004**, *16*, 537. b) J. Ding, J. Gao, Y. Cheng, Z. Xie, L. Wang, D. Ma, X. Jing, F. Wang, *Adv. Funct. Mater.* **2006**, *16*, 575. c) M. D. McGehee, T. Bergstedt, C. Zhang, A. P. Saab, M. B. O'Regan, G. C. Bazan, V. I. Srdanov, A. J. Heeger, *Adv. Mater.* **1999**, *11*, 1349. d) Y. L. Tung, S. W. Lee, Y. Chi, L. S. Chen, C. F. Shun, F. I. Wu, A. J. Carty, P. T. Chou, S. M. Peng, G. H. Lee, *Adv. Mater.* **2005**, *17*, 1095. e) S. Lamansky, P. Djurovich, D. Murphy, F. Abdel-Razzaq, H. E. Lee, C. Adachi, P. E. Burrows, S. R. Forrest, M. E. Thompson, *J. Am. Chem. Soc.* **2001**, *123*, 4304. f) R. C. Kwong, S. Sibley, T. Dubovoy, M. Baldo, S. R. Forrest, M. E. Thompson, *Chem. Mater.* **1999**, *11*, 3709. g) W. Y. Wong, G. J. Zhou, X. M. Yu, H. S. Kwok, B. Z. Tang, *Adv. Funct. Mater.* **2006**, *16*, 838. h) F. Li, M. Zhang, J. Feng, G. Cheng, Z. J. Wu, Y. G. Ma, S. Y. Liu, J. C. Sheng, S. T. Lee, *Appl. Phys. Lett.* **2005**, *83*, 365. i) X. Z. Jiang, A. K. Y. Jen, B. Carlson, L. R. Dalton, *Appl. Phys. Lett.* **2002**, *81*, 3125.

[5] a) C. Y. Jiang, W. Yang, J. B. Peng, S. Xiao, Y. Cao, *Adv. Mater.* **2004**, *16*, 537. b) X. Gong, S. H. Lim, J. C. Ostrowski, D. Moses, C. J. Bardeen, G. C. Bazan, *J. Appl. Phys.* **2004**, *95*, 948. c) F. Z. Shen, H. Xia, C. B. Zhang, D. Lin, L. He, Y. G. Ma, *J. Phys. Chem. B* **2004**, *108*, 1014. d) F. Z. Shen, H. Xia, C. B. Zhang, D. Lin, X. D. Liu, Y. G. Ma, *Appl. Phys. Lett.* **2004**, *84*, 55.

[6] a) M. H. Tsai, H. W. Lin, H. C. Su, T. H. Ke, C. C. Wu, F. C. Fang, Y. L. Liao, K. T. Wong, C. I. Wu, *Adv. Mater.* **2006**, *18*, 1216. b) K. T. Wong, Y. L. Liao, Y. T. Lin, H. C. Su, C. C. Wu, *Org. Lett.* **2005**, *7*, 5131. c) Y. C. Chen, G. S. Huang, C. C. Hsiao, S. A. Chen, *J. Am. Chem. Soc.* **2006**, *128*, 8549.

[7] a) S. C. Chang, G. F. He, F. C. Chen, T. F. Guo, Y. Yang, *Appl. Phys. Lett.* **2001**, *79*, 2088. b) F. C. Chen, G. F. He, Y. Yang, *Appl. Phys. Lett.* **2003**, *82*, 1006. c) T. H. Liu, S. F. Hsu, M. H. Ho, C. H. Liao, Y. S. Wu, C. H. Chen, *Appl. Phys. Lett.* **2006**, *88*, 063 508.

[8] M. Sudhakar, P. I. Djurovich, T. E. Hogen-Esch, M. E. Thompson, *J. Am. Chem. Soc.* **2003**, *125*, 7796.

[9] a) S. Tokito, T. Iijima, Y. Suzuri, H. Kita, T. Tsuzuki, F. Sato, *Appl. Phys. Lett.* **2003**, *83*, 569. b) V. Adamovich, J. Brooks, A. Tamayo, A. M. Alexander, P. I. Djurovich, B. W. D'Andrade, C. Adachi, S. R. Forrest, M. E. Thompson, *New J. Chem.* **2002**, *26*, 1171. c) G. T. Lei, L. D. Wang, L. Duan, J. H. Wang, Y. Qiu, *Synth. Met.* **2004**, *144*, 249. d) R. J. Holmes, B. W. D'Andrade, S. R. Forrest, X. Ren, J. Li, M. E. Thompson, *Appl. Phys. Lett.* **2003**, *83*, 3818. e) S. J. Yeh, M. F. Wu, C. T. Chen, Y. H. Song, Y. Chi, M. H. Ho, S. F. Hsu, C. H. Chen, *Adv. Mater.* **2005**, *17*, 285.

[10] Y. Y. Noh, C. L. Lee, J. Kim, K. Yase, *J. Chem. Phys.* **2003**, *118*, 2853.

[11] T. H. Kim, D. H. Yoo, J. H. Park, O. O. Park, J. W. Yu, J. K. Kim, *Appl. Phys. Lett.* **2005**, *86*, 171 108.

[12] A. Juris, V. Balzani, F. Barigelletti, S. Campagna, P. Belser, A. V. Zelewsky, *Coord. Chem. Rev.* **1988**, *84*, 85.

[13] S. Lunak, M. Nepras, R. Hrdina, A. Kurfurst, J. Kuthan, *Chem. Phys.* **1993**, *170*, 77.

[14] J. K. Lee, M. F. Rubner, *Appl. Phys. Lett.* **1996**, *69*, 1686.

[15] J. N. Demas, *J. Chem. Educ.* **1983**, *60*, 803.

[16] B. P. Sullivan, D. J. Salmon, T. J. Meyer, *Inorg. Chem.* **1978**, *17*, 3334.